On the Stability of Myosin Filaments*

Robert Josephs† and William F. Harrington

ABSTRACT: Previous work has established that myosin molecules are in rapid equilibrium with a single, high molecular weight polymeric species (mol wt 50–60 × 10^6) in the pH range 8–8.5 (KCl concentration 0.13–0.20 M). In the present study the equilibrium constant of this myosin–polymer system has been evaluated from sedimentation velocity experiments as a function of ionic strength, pH, temperature, and hydrostatic pressure. Results indicate that the transformation of myosin monomer into polymer is accompanied by the release of 11 moles of KCl/monomer unit while approximately 0.68 mole (per monomer) of hydrogen ion is absorbed. The equilibrium constant is independent of temperature (over the range 1–16°), but is markedly affected by hydrostatic pressure. The dependence of the equilibrium constant on the hydrostatic pressure generated in high-speed sedimentation experiments has been evaluated and from these studies a positive volume change of 380 cc/mole of monomer was estimated for the association process. These results, when taken in conjunction, suggest that a maximum of 25 ionic bonds (per myosin molecule) is formed when the monomeric units associate to form the ordered macrostructure of the polymer.

When the ionic strength of 0.5 M KCl solutions of myosin is lowered by dialysis or dilution, the monomeric units associate to form long, filamentous macrostructures (Jakus and Hall, 1947; Noda and Ebashi, 1960; Zobel and Carlson, 1963; Huxley, 1963; Kaminer and Bell, 1966a,b; Josephs and Harrington, 1966). Huxley's (1963) electron microscope investigations of the filaments formed at an ionic strength of 0.15 M near neutral pH reveal that, although this system is heterodisperse in length, individual particles have diameters of 100–150 Å, irregular surface projections, and a bare central region (of the order of 1500–2000 Å) strongly reminiscent of the morphological features of thick filaments observed in muscle fibers. Particles of similar topology but with a relatively sharp size distribution (Kaminer and Bell, 1966a,b; Josephs and Harrington, 1966) are generated in the pH range 8–8.5 (KCl = 0.10–0.20 M) and velocity sedimentation studies demonstrate that these synthetically prepared myosin filaments are in rapid, reversible equilibrium with monomeric myosin molecules in solution. Only two sedimenting boundaries are observed in the ultracentrifuge under these conditions: a hypersharp polymer peak with $s^0_{20,w}$ = 150 S and a slower sedimenting monomer peak with $s^0_{20,w}$ = 6.5 S. Results from electron microscope and hydrodynamic studies indicate that approximately 75–95 monomer units are associated to form the polymer.

We have already provided qualitative evidence that the myosin–polymer equilibrium is altered by variations in the ionic strength and pH and shows a striking dependence upon the hydrostatic pressure produced in high-speed centrifugation (Josephs and Harrington, 1966, 1967). In the work to be presented below the effect of these parameters on the monomer–polymer equilibrium constant is more fully documented, and it is shown that the results give considerable insight into the forces responsible for the stability of the myosin filament.

It seems likely from these studies and the recent reports of Kegeles *et al.* (1967) and TenEyck and Kauzmann (1967) that investigations on the effect of pressure on interacting systems can provide important additional information on the fundamental mechanisms underlying association processes.

Materials and Methods

Reagents. Glass-distilled water was used in all experiments. Mineral oil (Gilpin Co., no. 641391) was USP grade; all other reagents were analytical grade.

Preparation of Myosin Polymers. Rabbit myosin in 0.5 M KCl was prepared and polymerized by dialysis as previously described (Josephs and Harrington, 1966) and stored at 5° until use. All experiments reported here were carried out within 7 days after sacrificing the animal.

Mineral Oil Experiments. In certain ultracentrifuge experiments mineral oil was layered over protein solutions in order to increase the hydrostatic pressure at the solution–oil interface. The mineral oil was always equilibrated with dialysate of the protein solution prior to its introduction into the centrifuge cell. Schlieren patterns taken at high speed revealed the presence of very small positive concentration gradients in the oil layer indicating that a small amount of water dissolved in the oil. Negative concentration gradients on the solu-

* Contribution No. 532 from the Department of Biology, McCollum-Pratt Institute, The Johns Hopkins University, Baltimore, Maryland. *Received February 27, 1968.* This investigation was supported by U. S. Public Health Service Grant No. AM-04349. One of us (R. J.) gratefully acknowledges a postdoctoral fellowship from the National Cystic Fibrosis Research Foundation.

† Present address: Laboratory of Molecular Biology, Cambridge, England.

tion side of the interface, indicative of oil dissolved in the solution phase, were never observed.

The density of the mineral oil was 0.85 g/100 ml. The oil underwent less than 5% reduction in volume upon acceleration from 24,000 to 60,000 rpm.

Protein Concentration. Protein concentrations were determined spectrophotometrically prior to ultracentrifugation, as previously reported. At rotor velocities below 45,000 rpm, concentration profiles in the centrifuge cell were always determined utilizing the Rayleigh interference optical system and assuming that a shift of 40 fringes is equivalent to a concentration change of 1.0 g/100 ml in a 12-mm centerpiece. At higher rotor velocities concentrations were estimated from schlieren peak areas.

Ultracentrifugation. With the exception of experiments described to study the temperature dependence of the polymerization reaction, all ultracentrifugation studies were carried out at rotor temperatures near 5°. The experimental conditions have been previously described (Josephs and Harrington, 1966). Capillary-type synthetic boundary cells were used to facilitate determination of the concentration change across the monomer boundary for experiments performed at low rotor velocities (less than 13,000 rpm). This was of special importance in the studies of the pH, KCl, and temperature dependence of the equilibrium constant. Either 12- or 30-mm synthetic boundary cells were used, depending upon experimental conditions.

Absolute concentration gradients were calculated from schlieren patterns in conjunction with Rayleigh interference patterns. Since schlieren patterns record the relative concentration gradient, it is necessary to determine the proportionality factor relating the relative gradient to the absolute gradient. This factor is readily obtained by numerical differentiation of an interference pattern in a region of the cell where the gradient is not changing rapidly. The absolute gradient thus obtained is compared with the schlieren pattern at the same radial distance.

Measurements of distances on ultracentrifuge photographic plates were made with the aid of a Nikon Model 6 shadowgraph microcomparator.

Results

Equations describing the concentration profiles to be expected in a rapidly equilibrating, pressure-independent polymerizing system undergoing mass transport have been derived by Gilbert (1955, 1959). For a polymerization reaction

$$nM \rightleftharpoons P \tag{1}$$

the equilibrium constant, K, may be expressed as

$$K = \frac{c_p}{(c_m)^n} \tag{2}$$

where c_p is the concentration of polymer, c_m is the concentration of monomer, and n is the number of monomer units undergoing association to form the polymer. If concentrations are expressed in weight units (g/100 ml), then the appropriate equations are

$$c_m = \left(\frac{1}{nK} \times \frac{\delta}{1-\delta}\right)^{\frac{1}{n-1}} \tag{3}$$

$$c_p = K\left(\frac{1}{nK} \times \frac{\delta}{1-\delta}\right)^{\frac{n}{n-1}} \tag{4}$$

The parameter, δ, is the velocity of a point, x, referred to a frame of reference in which the monomer has zero velocity and the polymer unit velocity. If the velocity of the monomer and polymer relative to an external frame of reference are known, then δ is given by

$$\delta = \frac{s_x - s_m}{s_p - s_m} \tag{5}$$

where s_x is the velocity of point x, s_m and s_p are the velocities of the monomer and polymer, respectively, all referred to the same external frame of reference.

In applying eq 1–5 to a polymerizing system undergoing transport in the ultracentrifuge the velocities of the monomer and polymer are expressed as their respective sedimentation coefficients, and effects arising from diffusion, radial field, and concentration dependence of sedimentation are neglected. The errors implicit in this procedure have been discussed in detail by Gilbert (1955, 1959, 1963), Nichol *et al.* (1964), and Fujita (1962).

Concentration profiles for monomer–polymer equilibria are readily obtained by inserting values of K and n into eq 3 and 4, allowing δ to vary from 0 to a value approaching unity. The total concentration at any point, c_t, is $c_m + c_p$, and for each value of δ there is a corresponding value of c_t. Thus the maximum value of c_t defines the maximum value of δ.

In the present study values of c_m, c_p, and c_t have been expressed in weight units of grams per deciliter. Unless otherwise noted, these are always the concentration units used to calculate the equilibrium constant, K.

Figure 1 presents a plot of c_m, c_p, and c_t *vs.* δ, calculated from eq 3 and 4 with $n = 83$ and $K = 10^{50}$ assuming a molecular weight of the myosin monomer of 600,000 (Woods *et al.*, 1963) and that of the polymer of 50×10^6. These parameters are appropriate for the myosin monomer–polymer equilibrium at pH 8.3, 0.19 M KCl (Josephs and Harrington, 1967; see below). Two boundaries are apparent; a slow boundary at $\delta = 0$, and a fast boundary the location of which depends upon $c_{t_{max}}$. The main features of interest are the extremely small variation of c_m with δ, the very low polymer concentration for δ less than 0.90, and the position of the fast boundary, which is always located near $\delta = 1$. These unusual features, all of which contrast sharply with equilibrium systems studied heretofore, stem from the large value of n (see also Gilbert, 1959, p 385). If eq 3 is divided by eq 4 we obtain

$$\frac{c_m}{c_p} = \frac{n(1-\delta)}{\delta} \tag{6}$$

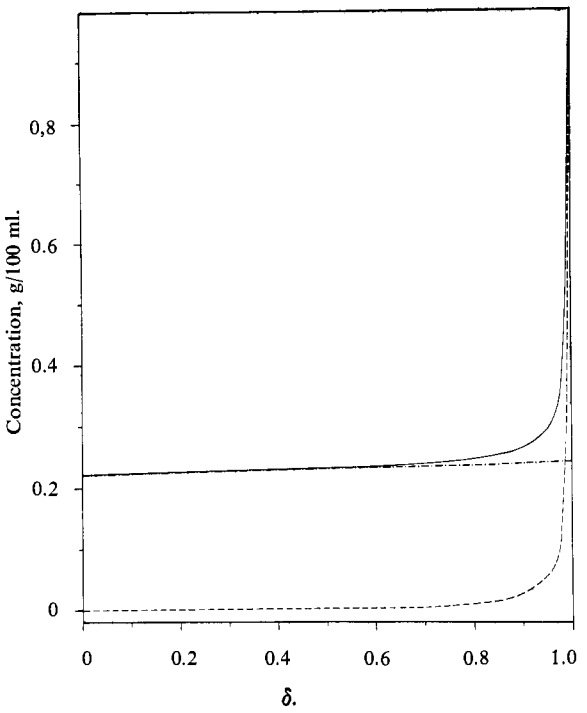

FIGURE 1: Concentration profile for the myosin monomer–polymer equilibrium (at pH 8.3, 0.19 M KCl) calculated from eq 3 and 4. $n = 83$ and $K = 10^{50}$. c_p (– – –), c_m (– · – · –), and c_t (——).

which can be rearranged to give

$$\delta = \frac{n}{\frac{c_m}{c_p} + n} \tag{7}$$

If $c_m/c_p \ll n$, then $\delta \rightarrow 1$. This is the situation most commonly encountered for the myosin–polymer system since, in order to have a readily measurable polymer concentration, c_m/c_p will be 5 or less, depending upon experimental conditions. Using the example in Figure 1, where $c_m/c_p = 5$, then $c_p = 0.06$ g/100 ml and $c_t = 0.36$ g/100 ml. The corresponding value of δ is 0.95. Higher protein concentrations will yield even lower ratios of c_m/c_p and δ values more closely approaching unity. Since the fast boundary is located at $\delta \rightarrow 1$, its observed sedimentation coefficient will closely approximate s_p.

The small variation of c_m with δ and c_p is also related to the high value of n. If c_m is calculated for two different values of δ, we obtain

$$\frac{c_{m_1}}{c_{m_2}} = \left(\frac{\delta_1(1-\delta_2)}{\delta_2(1-\delta_1)}\right)^{\frac{1}{n-1}} \tag{8}$$

Taking $\delta_1 = 0.15$ and $\delta_2 = 0.95$, which corresponds to points adjacent to the slow and fast boundaries, respectively, $c_{m_1}/c_{m_2} = 0.95$. Thus the monomer concentration increases by only 5% in the region between the two boundaries, whereas the polymer concentration increases by about 110-fold. These arguments show that the unusual features of this system result from large n, and are independent of K.

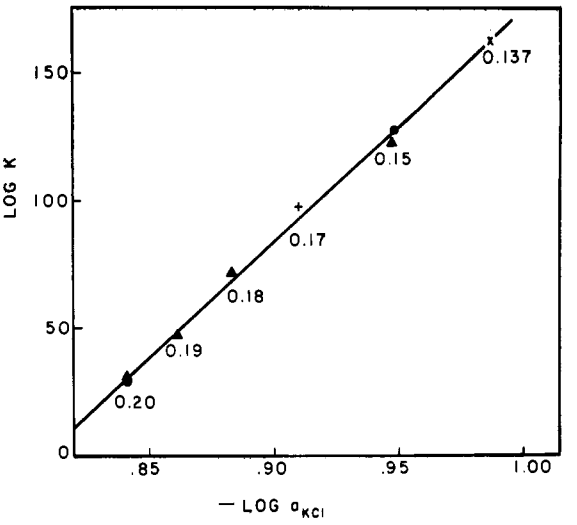

FIGURE 2: Plot of log K *vs.* $-\log a_{KCl}$. Different symbols represent different polymer preparations; the molarity of potassium chlroide is indicated below each experimental point. The pH of all protein solutions was maintained at 8.3 with 2×10^{-3} M Veronal buffer. Rotor velocities were between 9000 and 11,000 rpm.

The transformation of the c *vs.* δ plot into a radial concentration profile in a centrifuge cell requires a knowledge of s_m, s_p, and $c_{t_{max}}$ in addition to n and K. The positions of the slow and fast boundary may be arbitrarily chosen to give convenient resolution. Each radial position, x, between the two boundaries corresponds to a value of s_x and a value of δ which are related by eq 5. The concentration of monomer and polymer may then be obtained from eq 3 and 4.

Figure 1 demonstrates that the concentration change across the slow boundary very closely approximates the monomer concentration, c_m, while the concentration change across the fast boundary closely approximates the polymer concentration, c_p, and reveals that the concentration change between the boundaries is exceedingly small. Thus, the slow boundary may be identified as monomer and the fast boundary as polymer. From a knowledge of the concentration changes across the two boundaries, the equilibrium constant may be calculated from eq 2. Thus, paradoxically, this equilibrium system appears to behave as a mixture of two independent components.[1]

When Gilbert's equations are obeyed (eq 3–5) a plateau region exists on the fast side of the polymer boundary; the equilibrium constant may then be calculated directly from the observed concentration profile by

$$K = \frac{c_s^{1-n}(2n^2-2)^{n-1}(n-2)}{(2n^2-n)^n} \tag{9}$$

[1] The behavior of this equilibrium system differs from that of a mixture in that when two boundaries are observed the area under the slow boundary does not increase with increasing total protein concentration (see Josephs and Harrington (1966), Figure 13).

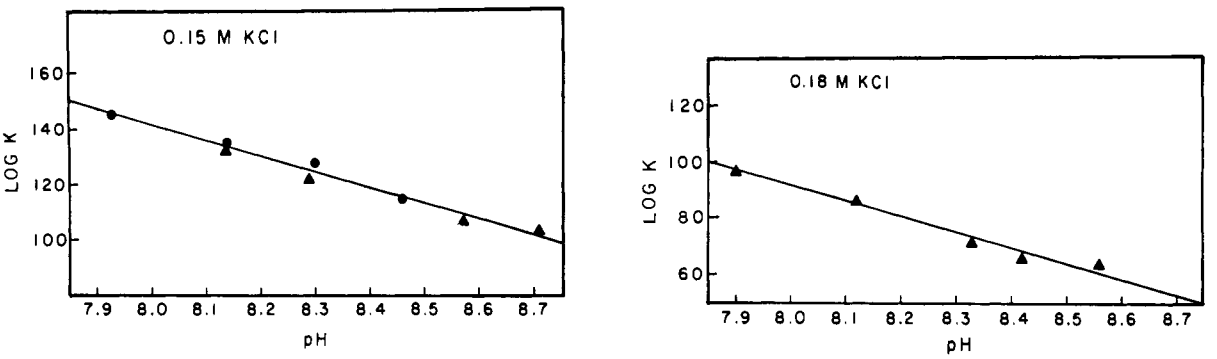

FIGURE 3: Plot of log K *vs.* pH at constant potassium chloride concentration. All protein solutions were buffered with 2×10^{-3} M Veronal at the desired pH. Rotor velocities were between 9000 and 11,000 rpm. (a) 0.15 M KCl and (b) 0.18 M KCl.

where c_s is the value of c_t at $\delta = (n - 2)/3(n - 1)$. For the myosin polymer system, $n = 83$, and the corresponding value of δ is 0.33. Because the polymer boundary is located very close to $\delta = 1$, c_s may be equated to the protein concentration at a point one-third of the distance between the monomer and polymer boundaries ($\delta = 0.33$). Precise positioning is not crucial, however, since only small (less than 0.02 g/100 ml) concentration changes occur in the region between the boundaries.

Experimentally, the most critical parameter required for determining K is an accurate measure of the concentration change across the slow boundary, since this is equated to c_m and raised to the power n (eq 2). In the present and previous studies, K has ranged from 10^{30} to 10^{150}. Because of the large value of n in the myosin–polymer system, it is desirable to use log K rather than K for the purpose of tabulation and comparison since the experimental error in determining c_m leads to a comparable error in log K; *i.e.*, for log $K = 50$, an error of 5% in c_m and c_p leads to an error of about 8% in log K but an error of 10^4 in K.

The Effect of Hydrogen Ion and Potassium Chloride Concentration on the Equilibrium Constant. Qualitative evidence that both the salt concentration and the pH have a decided influence upon the equilibrium constant for the polymerization of myosin has been presented in an earlier report (Josephs and Harrington, 1966). In order to ascertain whether the polymerization involves stoichiometric reaction of the protein component with potassium chloride and hydrogen ion the previous qualitative studies have been extended here to provide quantitative data (Figures 2 and 3).

Since the equilibrium constant is also dependent upon pressure (Josephs and Harrington, 1967) it is mandatory to carry out the quantitative studies of the salt and pH dependence at low rotor velocities.[2] At rotor velocities of 11,000 rpm or less, the effects of pressure on the mass distribution are inconsequential, thereby allowing the utilization of eq 9 for calculating the equilibrium constant.[3]

The dependence of the equilibrium constant on the concentration of H^+ and KCl is presented in Figures 2 and 3. In Figure 2 the logarithm of the equilibrium constant is plotted against the negative logarithm of the activity of the potassium chloride concentration. The experimental results summarized in Figure 3a were obtained from myosin solutions containing 0.15 M KCl plus 2×10^{-3} M Veronal, while those summarized in Figure 3b were obtained from myosin solutions in 0.18 M KCl plus 2×10^{-3} M Veronal.

If, by taking into account the salt and pH dependence, the polymerization reaction is expressed as

$$d\mathrm{H}^+ + n\mathrm{M} \rightleftharpoons \mathrm{P} + b\mathrm{KCl} \qquad (10)$$

where d is the number of moles of hydrogen ion and b, the number of moles of KCl participating in the polymerization reaction per mole of polymer, then an equilibrium constant, K', may be defined as

$$K' = \frac{(\mathrm{P})(a_{\mathrm{KCl}})^b}{(c_m)^n(a_{\mathrm{H}^+})^d} = K\frac{(a_{\mathrm{KCl}})^b}{(a_{\mathrm{H}^+})^d} \qquad (11)$$

where K is given by eq 2; a_{KCl} and a_{H^+} are thermodynamic activities of KCl and H^+, respectively. The constant K' differs from K in that it is independent of pH and KCl concentration.[4] As the equation is written, the protein species include the bound ions which are released upon polymerization. From eq 11, the slope of a plot of log K *vs.* log a_{KCl} ($(\delta \log K/\delta \log a_{\mathrm{KCl}})_{T,P,pH}$) yields the number of KCl molecules released upon formation of 1 mole of polymer from 83 moles of monomer. The slope of the linear plot depicted in Figure 2 corresponds to the liberation of 11 ± 1 moles of KCl for each mole of polymerized monomer. Similarly, $-(\delta \log K/\delta \mathrm{pH})_{T,P,\mathrm{KCl}}$ is equal to the number of hydrogen ions taken up upon polymerization of 1 mole of polymer. In Figure 3 both series of experiments yield identical slopes

[2] Methods to assay the influence of pressure on a polymerization reaction have been discussed (Josephs and Harrington, 1967).

[3] In practice eq 9 and 2 give essentially identical results.

[4] Equation 11 fixes the standard state of KCl and hydrogen ion at unit activity, whereas eq 2 does not. The choice of standard state is, of course, arbitrary, and convenience in treatment of experimental data often dictates which standard state is preferable. In the present case the use of eq 11 allows determination of the coefficients b and d.

TABLE I: The Effect of Temperature on the Equilibrium Constant for the Polymerization of Myosin.[a]

KCl Concn (M)	Temp (°C)	Log K
0.168	1.1	96.8
	5.9	95.1
	10.7	97.4
	16.5	95.5
0.196	2.1	40.9
	10.4	38.8
	16.2	39.3

[a] Equilibrium constants were calculated from eq 9 as described in the text. All protein solutions were buffered with 2×10^{-3} M Veronal (pH 8.3). Polymer solutions in 0.168 M KCl were examined in 30-mm double-sector synthetic boundary cells (total protein concentration = 0.13 g/100 ml). Polymer solutions in 0.196 M KCl were examined in 12-mm double-sector synthetic boundary cells (total protein concentration 0.7 g/100 ml).

from which we estimate an average of 0.68 ± 0.05 mole of H^+ is absorbed for each mole of monomer incorporated into the polymer. If protein concentrations are expressed as moles per liter, then the standard free-energy change per mole of polymer may be calculated from eq 11 and $\Delta F = -RT \ln K'$. (The conversion of K from weight units into molar units may be obtained from log K (molar) = log K (g/dl) + 390). The value of ΔF (at 5°) thus obtained is -1.8×10^5 cal/mole, referred to a standard state of unit activity for each reaction component in eq 11, and 55.6 M for water.

It is pertinent to note that the above calculations, as well as those in the succeeding sections, assume n constant and equal to 83 under all experimental conditions. The value of n was determined from previous studies of the molecular weight of the polymer (Josephs and Harrington, 1966) and monomer (Woods *et al.*, 1963; Kielley and Harrington, 1960). Errors in either determination will change the value of n and require (proportionate) revision in the calculated number of ions released or absorbed upon polymerization.

The desirability of actually determining the molecular weight of the polymer under differing conditions need hardly be mentioned. However, the attendant difficulties both in the application of theory and from an experimental point of view preclude rigorous determination of the polymer molecular weight in the presence of significant amounts of monomer.

Temperature Dependence of the Equilibrium Constant. The temperature dependence of the myosin–polymer equilibrium constant was examined at 11,000 rpm in capillary-type synthetic boundary cells, and equilibrium constants were calculated from eq 9 as described above. Polymer solutions, prepared by dialysis against a common buffered solvent, were introduced into the centrifuge cells at 5°. These were placed in a rotor at the desired temperature and incubated for 0.5 hr prior to ultracentrifugation.

Aliquots of polymer solution were centrifuged at several temperatures between 1 and 16°. Since the pH of the buffer solution (2×10^{-3} M Veronal) is temperature dependent, the reported values of log K were reduced to a common pH (8.3) by utilizing the data on the pH dependence of log K presented in the previous section. Table I summarizes results obtained at two different salt concentrations.

The data in Table I fail to indicate a consistent change in log K with temperature, the variation observed being within the range of experimental error in determining log K.

Pressure Dependence of the Equilibrium Constant. CALCULATION OF SEDIMENTATION PROFILES. The experiments described in the previous sections were carried out at speeds of 11,000 rpm or less. If rotor velocities greater than 15,000–30,000 rpm are used, then as the more rapidly sedimenting polymer boundary moves through the centrifuge cell positive concentration gradients develop in all regions of the cell centrifugal to the monomer boundary. The formation of these gradients is a consequence of the pressure dependence of the equilibrium constant, such that increasing pressure results in partial dissociation of the polymer into monomer.

The equations used for calculating concentration profiles at low rotor velocity (eq 3 and 4) were derived for K constant and independent of pressure, P. At the higher rotor velocities (above 15,000–30,000 rpm), the pressure gradient existing in the ultracentrifuge cell leads to large changes in K, c_m, and c_p, rendering eq 3 and 4 inapplicable. In the succeeding paragraphs we shall present an approximate method by which the pressure dependence of the equilibrium constant may be taken into account to calculate the sedimentation profiles to be expected for the myosin–polymer equilibrium.

When K is a function of pressure, $K(P)$ is still given by eq 2, and is related to pressure and radial position, x, by

$$\log K(P) = \log c_p - 83 \log c_m = \log K - \frac{M_p \Delta\bar{v}}{2.3RT}\left(P_0 + \frac{\rho\omega^2}{2}(x^2 - x_0^2)\right) \quad (12)$$

where P_0 is the hydrostatic pressure at the meniscus of the solution (x_0), K, the equilibrium constant at 1 atm, M_p, the molecular weight of the polymer (50×10^6), $\Delta\bar{v}$, the change in partial specific volume on polymerization, ρ, the density of the solution, and ω, R, and T, the rotor velocity, the gas constant, and the temperature, respectively.

For experimentally convenient situations log $c_p \ll 83 \log c_m$, and therefore the concentration profile of the monomer may be obtained from eq 12 without precise knowledge of c_p. For the purposes of calculation, the initial[5] (time zero) distribution of monomer and poly-

[5] The initial or zero-time distribution is the concentration profile of the reactants after the rotor has reached the desired angular velocity, but before significant mass transport has occurred.

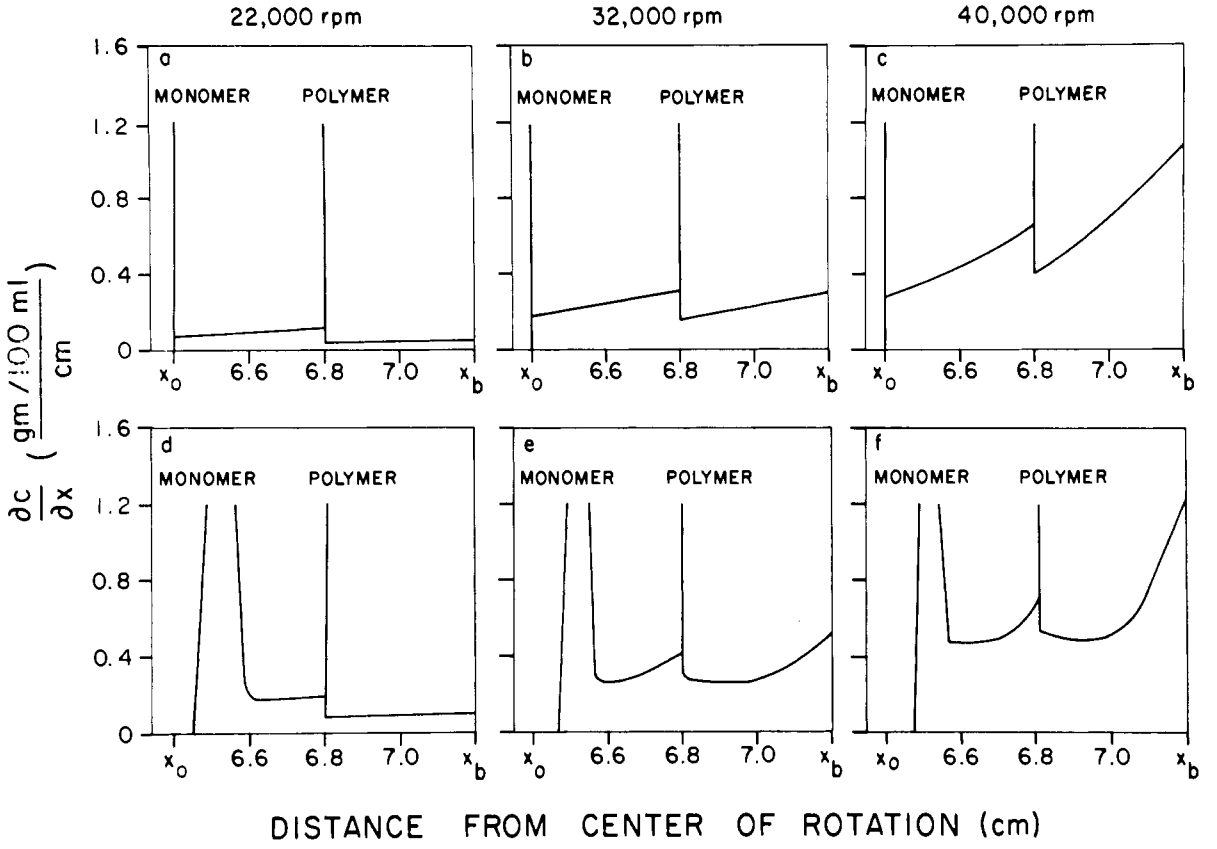

FIGURE 4: The effect of rotor velocity on calculated (a–c) and experimentally observed (d–f) schlieren patterns for the myosin polymer equilibrium system at pH 8.3, 0.18 M KCl; initial total protein concentration is 0.66 g/100 ml for all frames. (a–c) Patterns obtained by numerical differentiation of concentration profiles calculated from eq 12 (see text) with $M_p = 50 \times 10^6$, $T = 278°K$, $\log K = 71$, $\Delta\bar{v} = 6.8 \times 10^{-4}$ cc/g, $x_0 = 6.40$ cm, $\rho = 1.0$ g/ml, and $P_0 = 1$ atm. (d–f) Experimentally observed sedimentation profiles for the myosin polymer equilibrium ($T = 273°K$, $\log K = 71$, $\Delta\bar{v} = 6.8 \times 10^{-4}$ cc/g, and $x_0 = 6.4$ cm). Time of centrifugation: (d) 182 min, (e) 72 min, and (f) 46 min.

mer may be determined by assigning c_p at the meniscus any convenient value within the restriction $c_m/c_p < 5$ at every radial point within the liquid column. Then the initial polymer concentration at each radial position within the liquid column is the difference between the initial total concentration and the monomer concentration. According to arguments presented above, the large value of n renders c_m practically independent of c_p. Consequently, sedimentation of polymer will have a vanishingly small effect on the concentration profile of the monomer. Conversely, as long as eq 12 is satisfied for all regions of the cell, the polymer concentration profile will be sensibly unchanged during sedimentation, except for a small reduction in concentration due to radial dilution. Since $s_m \ll s_p$ further simplification in computing the mass distribution during sedimentation may be realized by holding the monomer boundary fixed at its initial position. The concentration profile calculated for a conventional sedimentation velocity experiment is the sum of c_p and c_m ($= c_t$) at each level in the cell, with c_m ($\approx c_t$) in the region centripetal to the polymer boundary. With these approximations, we have previously (Josephs and Harrington, 1967) presented concentration profiles depicting the progress of a sedimentation velocity experiment.

It is now of interest to explore the effect of varying the rotor velocity upon sedimentation profiles predicted by eq 12. For the purpose of comparison, the concentration gradient is a more sensitive and illustrative parameter than the concentration itself and may be readily obtained by numerical differentation of calculated concentration profiles. Figure 4a–c presents calculated concentration gradients (schlieren patterns) in which the polymer has sedimented from the meniscus (6.4 cm) to a position 6.8 cm from the center of rotation. The schlieren patterns were calculated for three rotor velocities, 22,000, 32,000, and 40,000 rpm, using experimentally determined values of M_p, T, $\log K$, and $\Delta\bar{v}$ (see below). Features common to all the patterns include the existence of a positive concentration gradient of varying magnitude in all regions of the cell. On either side of the polymer boundary the concentration gradient is increasing radially, the rate of increase being greater at higher rotor velocities. The concentration gradient is discontinuous at the polymer boundary, being greater on the centripetal than the centrifugal side.

Figure 4d–f shows the experimentally observed absolute concentration gradients which may be compared with those calculated and shown in frame 4a–c.

The unusual boundary shape displayed by the sedimentation patterns in Figure 4a–f is a singular result of the variation of the equilibrium constant with pres-

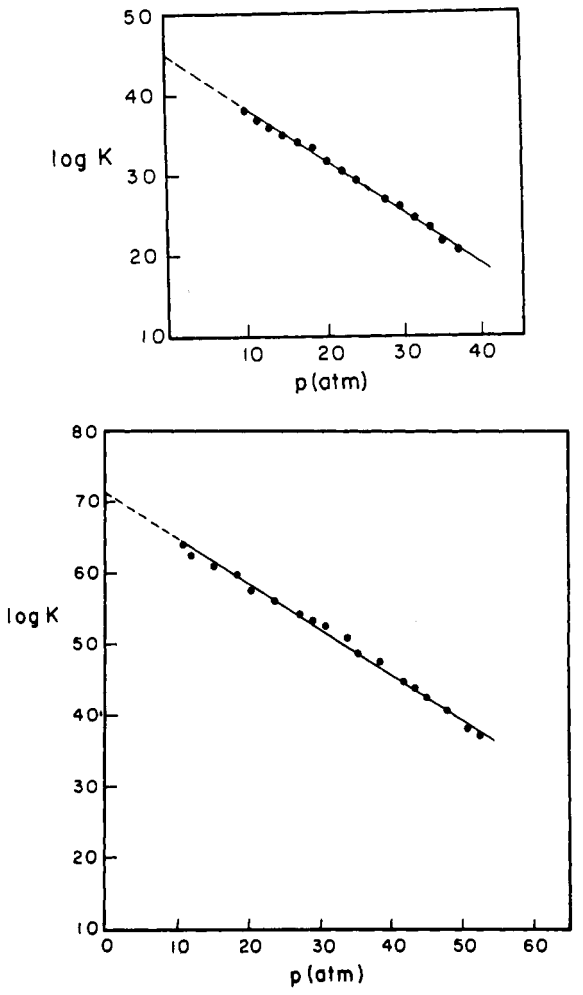

FIGURE 5: Plots of log K against hydrostatic pressure for the myosin monomer–polymer equilibrium. (a) Top: rotor velocity 22,000 rpm, KCl concentration 0.194 M; 2×10^{-3} M Veronal (pH 8.3); protein concentration is 1.0 g/100 ml. (b) Bottom: rotor velocity 32,000 rpm, KCl concentration 0.18 M; 2×10^{-3} M Veronal (pH 8.3); protein concentration 0.6 g/100 ml.

sure. The origin of the most salient features in both the calculated (a–c) and the experimental (d–f) patterns may be qualitatively understood in terms of the gradients generated by the "individual" sedimenting species. The total gradient at any point is then obtained as the algebraic sum of the positive monomer and the negative polymer gradients at the same point.

Considering first the gradient of the monomer concentration, we recall that previous studies (Josephs and Harrington, 1967) have emphasized that increasing hydrostatic pressure causes a shift in the equilibrium toward increasing monomer concentration. This property of the myosin equilibrium system is evidenced in two ways. At constant rotor velocity the pressure gradient ($\delta P/\delta x = \rho\omega^2 x$) increases with radial distance, and hence the monomer gradient undergoes a similar increase. The pressure gradient is much greater at higher rotor velocities, and therefore we would anticipate correspondingly greater monomer gradients at higher rotor velocity. In calculating the concentration gradients, the concentration of polymer centripetal to the polymer boundary is taken as zero (see above), and therefore the gradient (calculated) over this region of the sedimentation pattern is entirely that of the monomer. In Figure 4a–f, the experimentally observed and the calculated concentration gradients centripetal to the polymer boundary clearly reflect the effect of the increase in the pressure gradient, with both radial distance and rotor velocity.

The factors influencing the shape of the schlieren pattern centrifugal to the polymer boundary are more complex. In this region of the cell the monomer gradient continues to increase radially, but the polymer gradient is negative (rather than zero) and is decreasing radially (*i.e.*, becoming more negative; for example, see Figures 3 and 4 of Josephs and Harrington, 1967). Recalling that the shape of the polymer boundary is assumed not to change during sedimentation (except by radial dilution), then at any radial position the absolute magnitude of the negative polymer gradient will necessarily be less than that of the monomer gradient at the same radial position, resulting in a net positive gradient. This expectation is confirmed in Figure 4 for both the idealized (a–c) and the actual (experimental) (d–f) schlieren patterns.

As noted above, the polymer concentration gradient changes abruptly from zero to a negative value at the polymer boundary. This discontinuity is reflected in the calculated as well as in the experimentally obtained schlieren patterns by a sharp drop in the gradient on the centrifugal side of the polymer boundary. Thus we see that the main qualitative features delineated for the calculated gradients are also evident in the schlieren patterns of the experimental gradients.

The lack of rigorous theoretical treatment describing boundary shapes for pressure-dependent interacting systems in the ultracentrifuge (TenEyck and Kauzmann, 1967; Kegeles *et al.*, 1967) has necessitated the introduction of certain approximations to facilitate construction of the schlieren patterns in Figure 4a–c. It is useful at this point to briefly review the nature of some of the major approximations and to indicate, where possible, the limitations of their validity.

In calculating the shape of the schlieren profiles concentration-dependent sedimentation of monomer and polymer was not taken into consideration due to the complexity of the resulting equations. Since the sedimentation coefficients of both species are markedly concentration dependent, inclusion of these effects may result in modification of the calculated schlieren patterns, particularly in the region centrifugal to the polymer boundary, where it will be noted that significant differences between the shapes of the calculated and experimental patterns do exist. For similar reasons the influence of diffusion was not taken into account as playing an important role in determining the shape of the sedimentation patterns, although in view of the high molecular weight and asymmetry of the protein components involved, this last omission is less likely to lead to serious error.

Of greater consequence perhaps is the effect of keeping the monomer boundary fixed at its initial position. Sedimentation of the monomer may be considered

roughly equivalent to a radial displacement of the entire monomer gradient, with appropriate minor adjustments of the boundary shape due to radial dilution and the concentration dependence of the monomer sedimentation coefficient. Sedimentation of the monomer would result in a reduction in the monomer concentration at each radial position, and consequently some polymer would dissociate in order to maintain the monomer at the equilibrium concentration, thus effecting a reduction in the net gradient.

Finally, those simplifications in computation relating to treating the sedimentation of monomer and polymer as being mutually independent derive exclusively from the large value of n for the myosin–polymer equilibrium, and analogous treatments cannot be expected to hold for systems where n is small (Kegeles *et al.*, 1967).

The agreement between the main features of the calculated and the experimental sedimentation patterns lends confidence to the general approach used in their computation. However, in view of the approximations discussed above, the calculated schlieren patterns necessarily represent a qualitative rather than a quantitative description of the sedimentation profile. The utility of this type of qualitative description in the analysis of the experimental data will soon become evident.

Determination of the Volume Change upon Polymerization. The pressure dependence of the myosin–polymer equilibrium depicted in Figure 4 implies that an increase in volume occurs upon polymerization. The volume change involved may be evaluated from experimental data by plotting log $K(P)$ against pressure, the slope of the plot being equal to $\Delta\bar{v}M_p/2.3RT$.

In order to determine log $K(P)$ as a function of pressure it is necessary to measure the concentration of monomer and polymer as a function of radial distance (*i.e.*, at different hydrostatic pressure) in the liquid column. Inspection of typical sedimentation velocity profiles of the myosin–polymer system (for example, see Figure 7a or Figures 1 and 2 of Josephs and Harrington, 1967) reveals how this may be accomplished.

As can be seen, the polymer boundary exhibits a very high degree of self-sharpening. By virtue of the very steep gradient at the boundary, interference fringes recorded by the Rayleigh optical system stop abruptly (without turning up) at the hypersharp polymer peak, thereby virtually eliminating ambiguities regarding the actual position of the polymer boundary, or the extent of the region centripetal to it. Thus, definition of the region centripetal to the polymer boundary is unequivocal, and the radial position of the polymer peak may be precisely determined. The monomer concentration is then equated to the total protein concentration at a point immediately (0.02 mm) centripetal to the polymer boundary (where $c_t \approx c_m$) for different radial positions, x, of the polymer peak during sedimentation (see above). The values of c_m thus obtained closely correspond to the concentration of monomer in equilibrium with polymer at the polymer boundary.

At the polymer boundary c_P is roughly the difference between the initial monomer concentration at the meniscus and the total initial protein concentration. (The initial monomer concentration at the meniscus may be estimated from the concentration change across the major monomer peak extrapolated to the base line.) A more accurate estimate of the polymer concentration is unnecessary since even very large errors (five- to tenfold) in c_P will exert a negligible effect on log $K(P)$.

Thus the equilibrium constant for the polymerization reaction has been evaluated at various depths in the centrifuge cell, each corresponding to a particular hydrostatic pressure. Figure 5 presents plots of log $K(P)$ *vs.* pressure. The value of $\Delta\bar{v}$ calculated from the slopes of the curves in Figure 5 is 6.4×10^{-4} cc/g. Similar plots were obtained from a series of experiments in which the rotor velocity, protein concentration, and salt concentration were varied. In all cases the value of $\Delta\bar{v}$ was $6.5 \pm 1.0 \times 10^{-4}$ cc/g. The results of these experiments are summarized in Table II.

TABLE II: The Effect of Varying Experimental Conditions on $\Delta\bar{v}$.[a]

Protein Concn (g/100 ml)	KCl (mole/l.)	Rpm	Log K (1 atm)	$\Delta\bar{v} \times 10^4$ (cc/g)
0.6	0.180	40,000	69	5.38
0.6	0.180	32,000	70	6.02
0.6	0.180	20,000	72	7.45
0.4	0.180	32,000	72	5.98
0.9	0.180	32,000	69	6.92
0.4	0.176	22,000	78	6.82
1.0	0.196	22,500	36	7.66
1.0	0.192	22,000	45	7.13
0.7	0.187	22,000	58	5.54
1.0	0.194	28,000	45	6.36
1.0	0.194	22,000	45	6.39
0.26	0.145	33,450	142	5.92

[a] Values of $\Delta\bar{v}$ were obtained from the slope of plots of log $K(P)$ *vs.* pressure ($= \Delta\bar{v}M_p/2.3RT$), similar to those in Figure 5. Log K (1 atm) was estimated by extrapolation of the same plots to 1 atm. Solutions were buffered with 2×10^{-3} M Veronal (pH 8.3). Other pertinent experimental conditions are indicated in the table.

The procedure for determining log $K(P)$ described above is imprecise to the extent that the observed concentration gradients are attributable to processes other than the pressure dependence of the monomer $\rightleftharpoons$ polymer equilibrium. For example, the generation of salt or pH gradients within the liquid column during ultracentrifugation may cause changes in the equilibrium constant unrelated to the effects of pressure. However in this instance interpretative difficulties may be minimized by utilizing experimental data recorded early in the experiment (before sufficient time has elapsed for significant distribution of the salt to occur) or near the

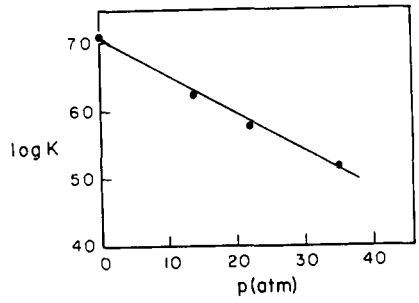

FIGURE 6: Plot of log K at zero time against hydrostatic pressure at the protein solution meniscus for myosin monomer–polymer equilibrium (see text for details): 0.18 M KCl; 2×10^{-3} M Veronal (pH 8.3); protein concentration 0.6 g/100 ml.

center of the liquid column, where the salt concentration is invariant with time.[6]

Additionally, while the arguments presented in part of this section have not considered the possibility of convective disturbances, calculations by Kegeles *et al.* (1967) show that under certain circumstances convection may occur during sedimentation of pressure-dependent equilibrium systems.

The significance of these effects as well as those discussed in the preceding section could be evaluated if the pressure dependence of the equilibrium constant were measured at zero time,[5] before any mass transport could occur. We have effected this measurement in the following manner. The equilibrium constant at the meniscus (*i.e.*, at zero time) was obtained by extrapolation of plots of log $K(P)$ *vs.* pressure similar to those presented in Figure 5 to the pressure prevailing at the protein solution meniscus. Normally this pressure is very close to 1 atm. However, the pressure at the meniscus can be varied independently of other experimental parameters through the expedient of placing a layer of mineral oil over the protein solution. Schlieren patterns obtained from this type of experiment have been published previously (Josephs and Harrington, 1967). The pressure at the meniscus was calculated from the density of the mineral oil (0.85 g/cc) and the positions of the oil–air and oil–solution menisci. By varying the thickness of the oil layer, values of log $K(P)$ have been obtained at the meniscus as a function of pressure at zero time. These data are presented in Figure 6 and Table III for a series of experiments carried out at a rotor velocity of 32,000 rpm. The partial specific volume change, $\Delta\bar{v}$, calculated from the slope of this plot is 6.2×10^{-4} cc/g, in good agreement with the average value estimated in Table II. Similar results were obtained from a set of experiments carried out at 40,000 rpm. Thus, although the sources of error discussed above must certainly exist, their effect on the determination of $\Delta\bar{v}$ lies within the range of the experimental error.

The summary of data already presented in Table III includes experiments in which the rotor velocity, protein concentration, and salt concentration was varied. As can be seen from the table, the value of $\Delta\bar{v}$ appears to be insensitive to variations in these experimental parameters.

TABLE III: The Effect of Varying Hydrostatic Pressure at the Oil–Solution Meniscus on Log K_m, Log K (1 atm), and $\Delta\bar{v}$.[a]

Pressure at the Meniscus (atm)	Log K (meniscus)	Log K (1 atm)	$\Delta\bar{v} \times 10^4$ (cc/g)
1	71	71	6.2
13.8	62	71	6.2
21.8	58	71	5.6
35.0	54	72	5.3

[a] Mineral oil was layered over protein solutions (protein concentration = 0.6 g/100 ml, 0.18 M KCl, and 2×10^{-3} M Veronal (pH 8.3)) prior to ultracentrifugation at 32,000 rpm. The hydrostatic pressure exerted by the layer of oil (at the protein solution meniscus) was calculated from the density of the oil (0.85 g/ml) and the measured position of the oil–air and oil–solution menisci. Extrapolation of plots of log $K(P)$ *vs.* pressure to the pressure prevailing at the solution meniscus (column 1) yielded log K (meniscus). Further extrapolation to 1 atm yielded log K (1 atm) and the value of $\Delta\bar{v}$ was estimated from the slope ($=\Delta\bar{v}M_p/2.3RT$).

Formation of a Differential Boundary upon Increasing the Rotor Velocity. In our earlier report we demonstrated the effect of increasing the rotor velocity from 33,000 to 60,000 rpm after the polymer boundary had sedimented through approximately half of the liquid column. The shift in equilibrium constant due to the increased hydrostatic pressure produced a splitting of the hypersharp polymer boundary resulting in the appearance of a slower sedimenting differential monomer boundary. A quantitative analysis of this phenomenon was rendered impractical due to the continual depletion of the polymer boundary as it sedimented into regions of increasing hydrostatic pressure. This process in turn led to the formation of increasing concentration gradients in all regions of the cell between the monomer and the polymer boundaries. This difficulty has now been circumvented by placing a layer of mineral oil over the protein solution. At low speed (24,000 rpm) the pressure perturbation of the equilibrium is too small to generate significant concentration gradients in the region between the monomer and polymer peaks as shown in Figure 7a. However, after increasing the rotor velocity to 60,000 rpm, the mineral oil layer exerts a pressure of 130 atm at the solution–oil interface. This additional increase in pressure upon acceleration is sufficient to cause *complete* dissociation of the polymer into monomer. No significant concentration gradients are evident except in the region of the original monomer boundary and at the position of the transformed polymer boundary which

[6] If a salt gradient great enough to effect significant changes in log $K(P)$ were present then we might expect the values of $\Delta\bar{v}$ obtained under differing experimental conditions to vary in a manner reflecting the changing salt gradient. Examination of the data in Table II fails to reveal any such variation.

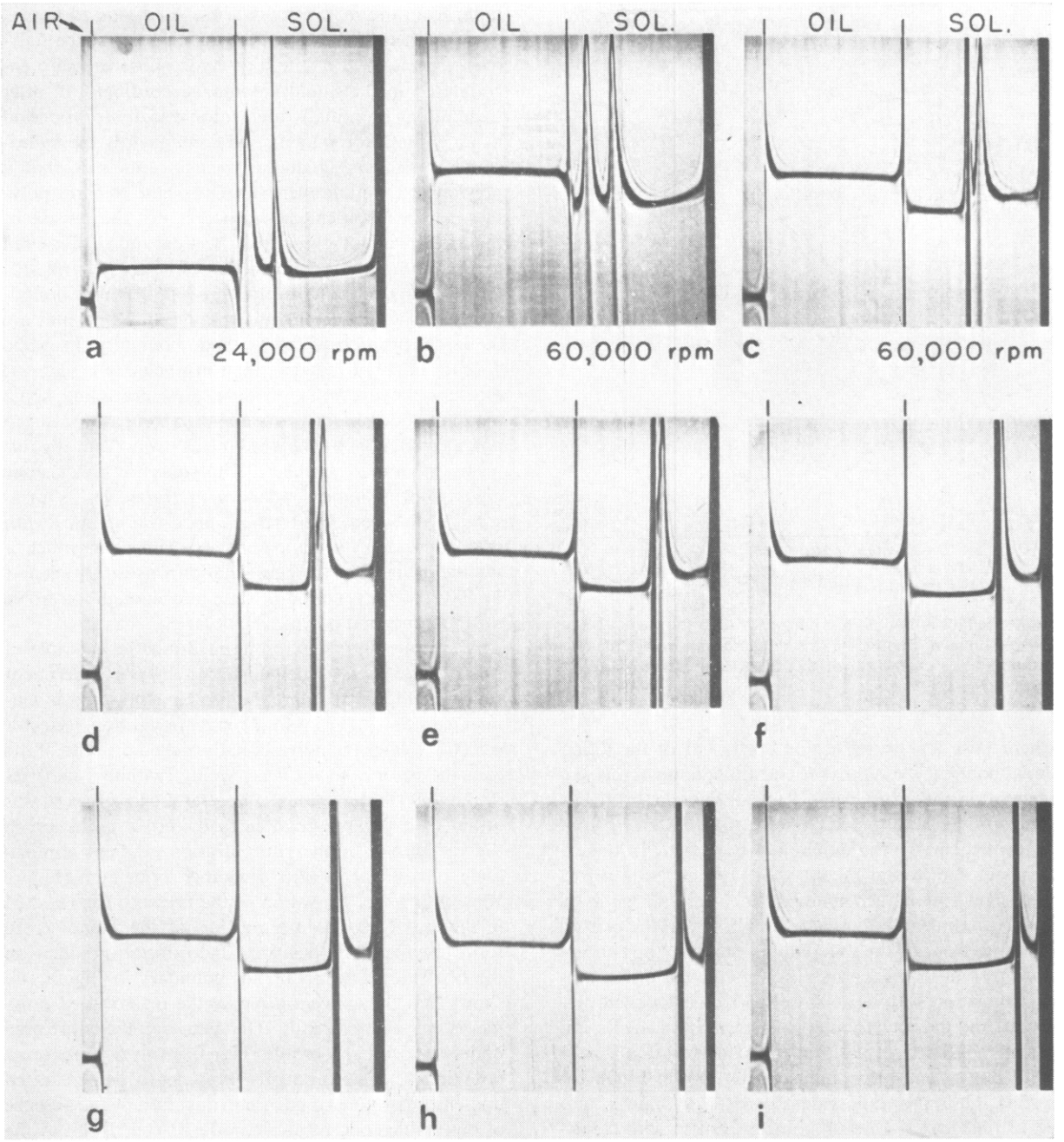

FIGURE 7: Sedimentation profiles demonstrating the formation of a differential monomer boundary upon increasing the rotor velocity from 24,000 to 60,000 rpm (see text for details). Protein concentraton 0.56 g/100 ml, in 0.18 M KCl, 2×10^{-3} M Veronal (pH 8.3).

is converted completely into a differential monomer boundary. The effect of the increased pressure is shown in Figure 7b–e, where it will be seen that the original monomer boundary sediments more rapidly than the transformed polymer boundary since the distance between the two schlieren peaks is closing. Frame f–i demonstrates that after a sufficient period of time the monomer boundary overtakes the differential boundary and merges with it, and subsequently only a single boundary is observed. This process is illustrated graphically in Figure 8 which presents a conventional log x *vs.* time plot, from which the sedimentation coefficient of the differential boundary was estimated to be 3.6 S, while that of the original monomer boundary was 5.4 S. After the two boundaries have merged, the sedimentation coefficient of the single resulting peak is 4.4 S.

The mechanism by which the boundary at the meniscus overtakes and merges with the differential boundary has been described in detail by Schachman (1959). The sedimentation coefficient of the differential boundary is related to the concentrations and sedimentation rates of the sedimenting species according to the equation

$$s_D = \frac{c_2 s_2 - c_1 s_1}{c_2 - c_1} \qquad (13)$$

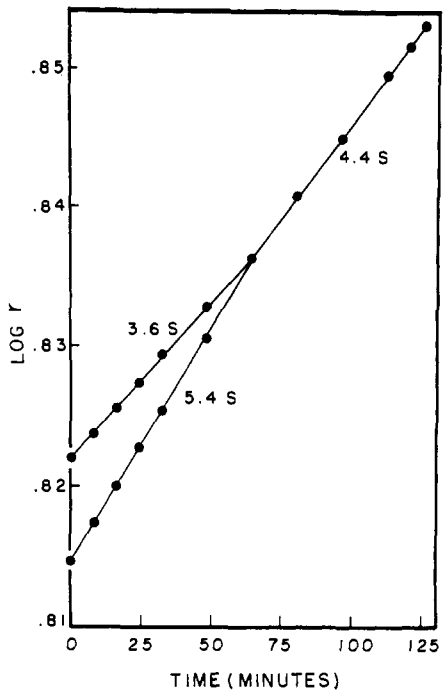

FIGURE 8: Plot of log radius *vs.* time for an experiment similar to that shown in Figure 7. The sedimentation coefficients corresponding to each limb of the curve are indicated in the figure.

where s_D is the sedimentation coefficient of the differential boundary, c is the concentration, and s is the sedimentation rate. Subscripts 1 and 2 refer, respectively, to the protein solution behind (centripetal) and in front of (centrifugal to) the differential boundary. In the experiment depicted in Figure 8 the concentration across the original monomer boundary, c_1, was 0.13 g/100 ml and the sedimentation rate, s_1, was 5.4 S. In the plateau region in front of the differential boundary the concentration of the original protein solution (c_2) prior to ultracentrifugation is 0.52 g/100 ml (corrected for radial dilution) and the corresponding sedimentation coefficient, s_2, for monomeric myosin at this concentration is 4.15 S (Chung *et al.*, 1967; Johnson and Rowe, 1960). Inserting the appropriate values of c_1, s_1, c_2, and s_2 into eq 13 yields $s_D = 3.7$ S, in good agreement with the experimental value of $s_D = 3.6$ S. The single peak observed after the original monomer boundary overtakes and merges with the differential boundary is a conventional boundary. Taking into account additional radial dilution, the concentration change across this boundary is 0.48 g/100 ml, and the sedimentation coefficient of myosin at this concentration, 4.3 S, closely agrees with the observed value, 4.4 S.

The agreement between the experimentally observed and the theoretically predicted values of s_D lends support to the original thesis that a differential monomer boundary is formed on increasing the rotor velocity, and that its formation is due to the pressure dependence of the equilibrium constant of the polymerization reaction.

Reassociation of the Monomer upon Reducing the Rotor Velocity. At high rotor velocities positive concentration gradients form in regions of the centrifuge cell remote from the major boundaries. As discussed above, these gradients result from the dissociation of the polymeric species due to the high hydrostatic pressure encountered in the liquid column. Accordingly, if, after maintaining an initially high rotor velocity for a period of time, the rotor velocity and consequently the hydrostatic pressure are reduced, we may anticipate that a portion of the monomer will reassociate to form polymer. This experiment, in essence, is just the reverse of that described in the preceding section and is presented in Figure 9. Frame 9a,b shows schlieren patterns obtained at 44,000 rpm in a capillary-type synthetic boundary cell. The vertical arrows over each frame indicate the initial position of the synthetic boundary. In frame 9c–e the effect of reducing the rotor velocity is seen. At the lower hydrostatic pressure now prevailing some monomer does, in fact, reassociate to form a hypersharp polymer boundary which sediments away from the diffusing monomer boundary. The concentration change across the monomer boundary in frame 9e, as measured by Rayleigh interference optics, was identical with that obtained in a companion experiment in which a sample of the same protein solution was centrifuged at 11,000 rpm for a period of time long enough to resolve the monomer and polymer boundaries.

A similar, and perhaps more dramatic, example of this phenomenon is demonstrated by the experiment shown in Figure 10. Here the protein solution was sedimented at 40,000 rpm in a conventional double-sector cell (10a). After the polymer had reached the base of the cell, the rotor velocity was rapidly (within 5 min) reduced to 9000 rpm. About 5 hr after the lower speed was attained, it became possible to discern a reduction in the magnitude of the concentration gradient immediately centrifugal to the monomer boundary (Figure 10b). As before, relaxation of the pressure has resulted in the reassociation of a portion of the monomer to form polymer. The positive concentration gradient on the fast side of the monomer boundary in Figure 10b shows that the concentration of the reassociated polymer is increasing radially. That is to say, the entire area under the schlieren profile centrifugal to the monomer boundary represents polymer as is clearly demonstrated upon more prolonged ultracentrifugation by the absence of detectable concentration gradients centripetal to the polymer boundary (frame c–f). Since the sedimentation coefficient of the polymer is strongly concentration dependent, the radial increase in polymer concentration must result in a radial decrease in sedimentation rate across the boundary. This situation leads to a pileup of mass as the rapidly sedimenting particles in the upper, dilute solution overtake those sedimenting at higher protein concentration in the lower solution, and accounts for the striking buildup of the polymer boundary observed in Figure 10d–f.

Discussion

The most striking feature of the present findings is the inordinate effect of pressure on the equilibrium constant of the myosin–polymer system. As we have seen, the change in the partial specific volume, $\Delta\bar{v}$, which oc-

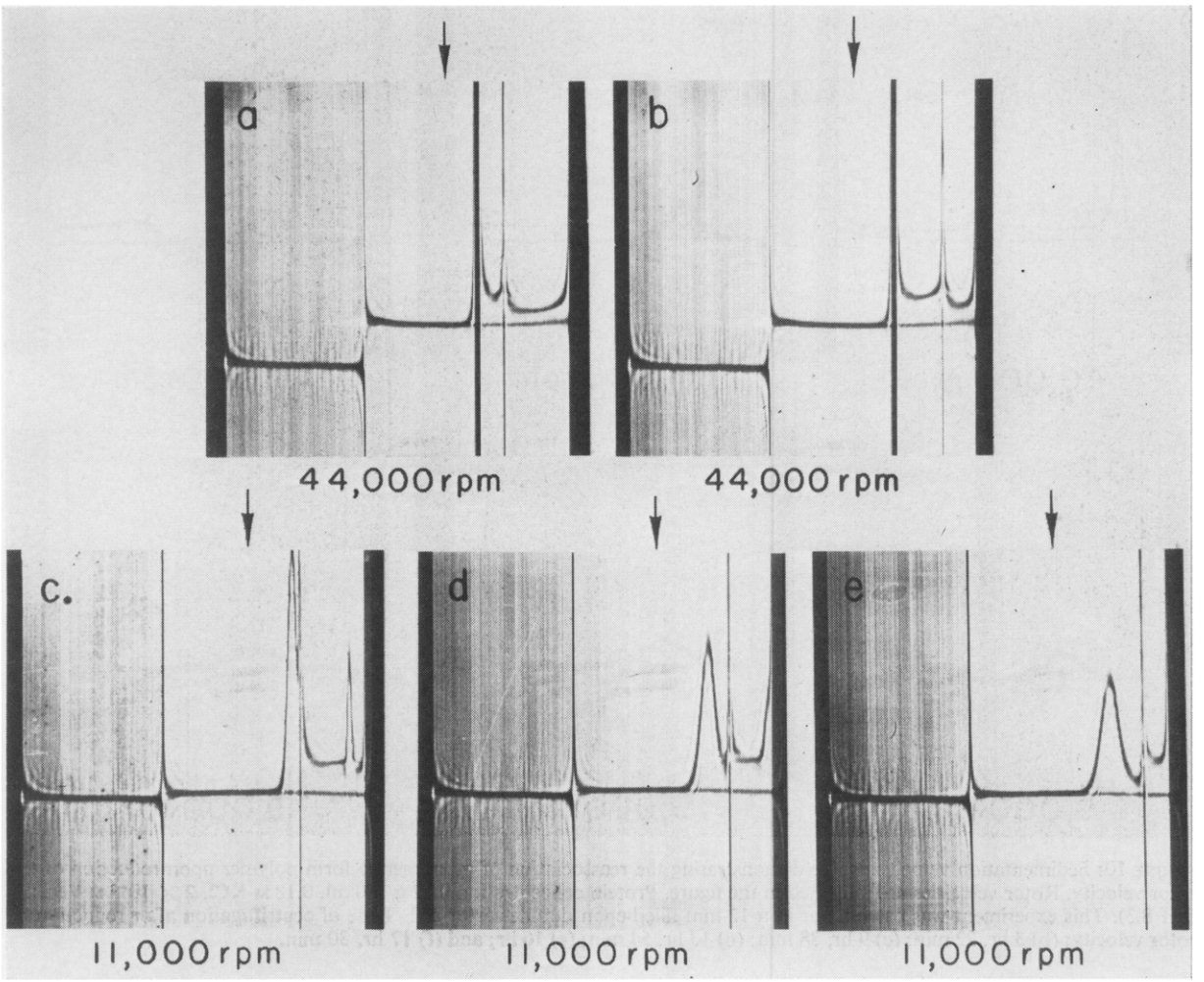

FIGURE 9: Sedimentation profiles demonstrating the reassociation of monomer to form polymer upon reduction of the rotor velocity. Rotor velocities are indicated in the figure. Protein concentration 0.76 g/100 ml in 0.19 M KCl, 2×10^{-3} M Veronal (pH 8.3). This experiment was carried out in a 12-mm double-sector capillary-type synthetic boundary cell. The vertical arrow in each frame indicates the position at which the synthetic boundary was formed. Time of centrifugation at 44,000 rpm: (a) 16 min, (b) 32 min. Time of centrifugation after reduction of the rotor velocity to 11,000 rpm: (c) 37 min, (d) 133 min, (e) 227 min.

curs during self-association of the monomeric species is of the order of 6.5×10^{-4} cc/g which corresponds to a positive volume change of 350–400 ml for each mole of myosin transformed into polymer. In seeking the origin of this volume change, we are led to consider both hydrophobic and ionic type bonding since it is likely that one or both of these forces are predominantly responsible for the stabilization of the filament. As Kauzmann (1959) has emphasized, in association reactions brought about either by hydrophobic or ionic bonding, $\Delta\bar{v}$ could be of the order of 10–20 ml/bond, and would be positive. Both ionic linkages and hydrophobic bonds are stabilized primarily by entropic effects and the volume change results from release of bound water on formation of the bond. In the case of the myosin system, ionic bonding would seem to play an important role in the association process since the stability of the filament is markedly depressed on addition of salt. At pH 8.3, 0.137 M KCl, nearly all of the myosin is present in polymeric form. When the salt concentration is increased to 0.22 M, virtually all of the polymer is transformed into monomer (Josephs and Harrington, 1966). In general, an elevation in the concentration of electrolytes tends to strengthen hydrophobic bonds as a result of the decreased solubility of nonpolar groups with increasing polarity of the solvent.

The apparent lack of a temperature dependence of the equilibrium constant (Table I) also favors the view that the association reaction is brought about primarily by ionic bonding. Since $d \ln K/d(1/T) = -\Delta H/R$, the enthalpy change for the association reaction must be close to zero. Hydrophobic bonding between aliphatic side chains is expected to show small positive enthalpies of formation, often with an enthalpy increase of up to 2 kcal/mole (Kauzmann, 1959; Scheraga, 1963), whereas ionic bonding is generally characterized by small heat effects and the driving force for the formation of such linkages lies entirely in the entropy change. Nevertheless, we cannot categorically exclude hydrophobic bonding, and an appreciable fraction of the bonds formed could be of this type.

We assume, then, that the positive volume change observed in the monomer–polymer transition results predominantly from the release of compressed water

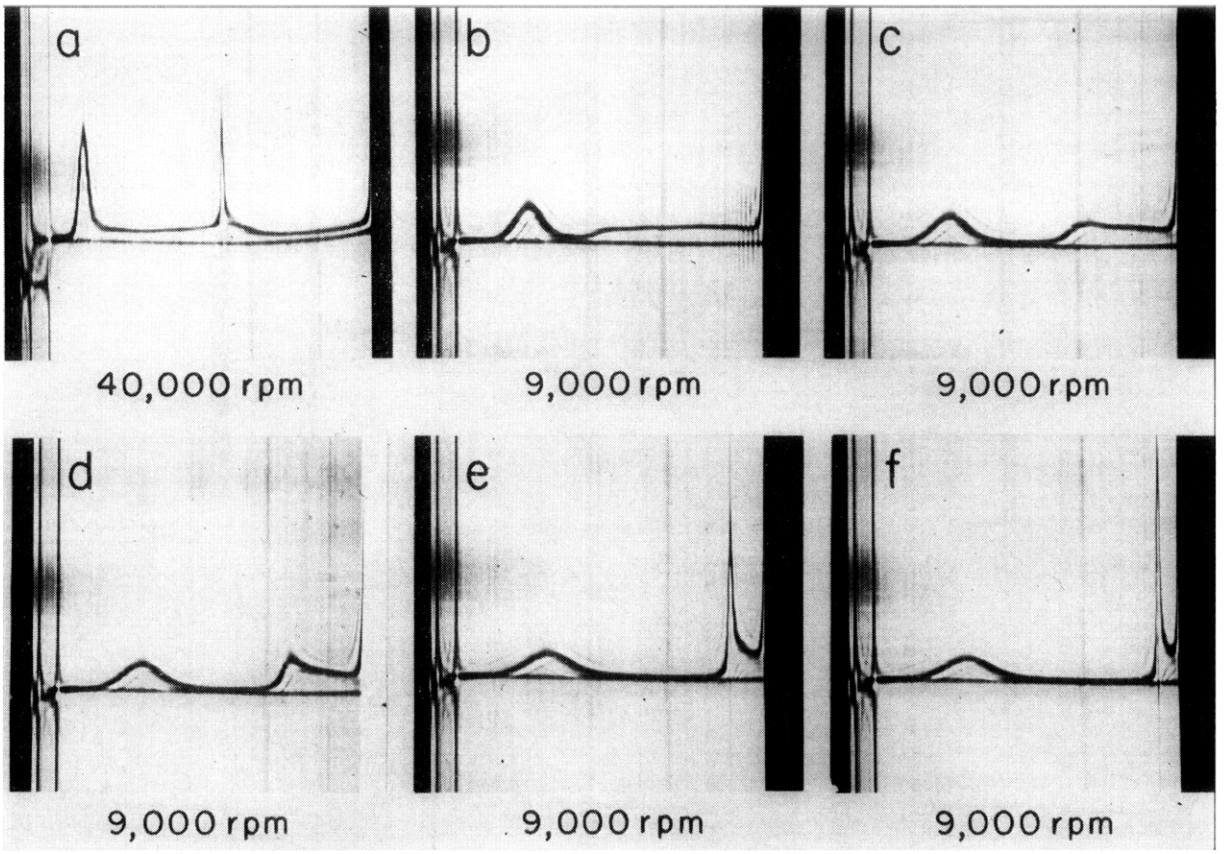

FIGURE 10: Sedimentation velocity profile demonstrating the reassociation of monomer to form polymer upon reduction of the rotor velocity. Rotor velocities are indicated in the figure. Protein concentration 0.62 g/100 ml, 0.18 M KCl, 2×10^{-3} M Veronal (pH 8.3). This experiment was carried out in a 12-mm filled-epon double-sector cell. Time of centrifugation after reduction of rotor velocity: (b) 5 hr, 22 min; (c) 9 hr, 38 min; (d) 13 hr, 54 min; (e) 16 hr; and (f) 17 hr, 30 min.

about certain of the charged groups on the surface of the myosin molecules when these associate to form the ordered macrostructure of the polymer. Accepting a value of 10–20 ml/bond (Kauzman, 1959), about 25 bonds, the major fraction ionic, will be formed in the reaction per mole of monomeric myosin. Although it is difficult to estimate precisely the entropy change related to this process in proteins, the average gain in unitary entropy per mole of ionic bonds formed in simple aqueous systems is in the range of 20–30 eu (Kauzmann, 1959). Thus the negative unitary free energy change ($\Delta F_u = -T\Delta S_u$) could be of the order of 140–210 kcal on transferring the monomer into polymer at 5°.

The data presented in Figures 2 and 3 are consistent with the view that both hydrogen ion and potassium chloride bear a fixed stoichiometric relationship to the protein components and therefore may be regarded, from a thermodynamic point of view, as reacting species. Accordingly, an equilibrium constant, K', independent of both pH and salt concentration, was determined from eq 11 and a free energy of polymerization (179 kcal/mole of polymer) could be estimated. It may be noted here that many polymerizing protein systems which are sensitive to salt concentration or pH do not exhibit stoichiometric relationships between the small ion and protein components (Steinhardt and Beychok, 1964). In these instances the sensitivity of polymerization to added ions is often attributed to alterations in the charge density or to changes in conformation of the interacting protein species. Since the equilibrium expression of eq 11 incorporates both salt and pH effects it is not necessary to invoke these arguments. In addition, the potassium binding of myosin has been measured by Lewis and Saroff (1957) and Mihalyi (1950). These authors report the binding of 250–300 ions/mole of monomer (based on a molecular weight of 600,000). Thus the formation of even as many as 25 ionic bonds with the concomitant liberation of 11 moles of KCl would not represent an unduly large change in the charge distribution.

On the basis of the electron microscope and hydrodynamic evidence cited in the beginning of the paper, it appears that the quaternary organization of the monomeric myosin molecules within the polymeric species ($s^0_{20,w} = 150$ S) is closely similar to that of the thick filament of muscle. According to current ideas (Huxley, 1963; Pepe, 1967a,b), the myosin molecules are oriented in antiparallel (tail-to-tail) array in the bare central region of the filaments and in parallel (head-to-tail) array in the corrugated surface regions. In Pepe's (1967a,b) model of the filament there are 12 rows of myosin molecules in a cross section in the bare central region (M-line region) and 18 rows in a cross section in the corrugated-surface regions. Individual molecules

are packed so that a triangular profile is obtained in cross section with three centrally located molecules surrounded by nine molecules on the surface. It is reasonable to expect that the water layer which surrounds the three interior molecules in their monomeric state may be reduced somewhat during association to allow close packing. As we have discussed above, the release of water is probably associated with the formation of ionic and possibly hydrophobic bonds.

An intriguing feature of the filament studies is the fact that 24 myosin molecules (those making up the bare central region) have a different packing arrangement than the remainder. This means that, in the polymeric species, about 30% of the molecules is packed in antiparallel array and about 70% in parallel array. This packing scheme correlates with the stoichiometry of the protons bound per myosin monomer (0.68 ± 0.05 mole of H^+) on transformation into polymer.

References

Chung, C.-S., Richards, E. G., and Alcott, H. S. (1967), *Biochemistry 6*, 3154.

Fujita, H. (1962), Mathematical Theory of Sedimentation Analysis, New York, N. Y., Academic, p 194.

Gilbert, G. A. (1955), *Discussions Faraday Soc. 20*, 68.

Gilbert, G. A. (1959), *Proc. Roy. Soc. (London) A250*, 377.

Gilbert, G. A. (1963), *Proc. Roy. Soc. (London) A276*, 354.

Huxley, H. E. (1963), *J. Mol. Biol. 7*, 281.

Jakus, M. A., and Hall, C. E. (1947), *J. Biol. Chem. 167*, 705.

Johnson, P., and Rowe, A. J. (1960), *Biochem. J. 74*, 432.

Josephs, R., and Harrington, W. F. (1966), *Biochemistry 5*, 3474.

Josephs, R., and Harrington, W. F. (1967), *Proc. Natl. Acad. Sci. U. S. 58*, 1587.

Kaminer, B., and Bell, A. L. (1966a), *Science 152*, 323.

Kaminer, B., and Bell, A. L. (1966b), *J. Mol. Biol. 20*, 391.

Kauzmann, W. (1959), *Advan. Protein Chem. 14*, 1.

Kegeles, G., Rhodes, L., and Bethune, J. L. (1967), *Proc. Natl. Acad. Sci. U. S. 58*, 45.

Kielley, W. W., and Harrington, W. F. (1960), *Biochim. Biophys. Acta 41*, 401.

Lewis, M. S., and Saroff, H. H. (1957), *J. Am. Chem. Soc. 79*, 2112.

Mihalyi, E. (1950), *Enzymologia 14*, 224.

Nichol, L. W., Bethune, J. L., Kegeles, G., Hess, E. L. (1964), *Proteins 2*, 305.

Noda, H., and Ebashi, S. (1960), *Biochem. Biophys. Acta 41*, 386.

Pepe, F. (1967a), *J. Mol. Biol. 27*, 203.

Pepe, F. (1967b), *J. Mol. Biol. 27*, 227.

Schachman, H. K. (1959), Ultracentrifugation in Biochemistry, New York, N. Y., Academic.

Scheraga, H. A. (1963), *Proteins 1*, 477.

Steinhardt, J., and Beychok, S. (1964), *Proteins 2*, 139.

TenEyck, L. F., and Kauzmann, W. (1967), *Proc. Natl. Acad. Sci. U. S. 58*, 888.

Woods, E. F., Himmelfarb, S., and Harrington, W. F. (1963), *J. Biol. Chem. 232*, 2374.

Zobel, C. R., and Carlson, F. D. (1963), *J. Mol. Biol. 7*, 78.